University of North Carolina Asheville
Journal of Undergraduate Research
Asheville, North Carolina
November 2020

Effects of Exit Channel Variants on Proton Translocation in E. coli ATP Synthase

Benjamin Pressley
Biology
University of North Carolina Asheville
One University Heights
Asheville, North Carolina 28804 USA

Faculty Advisor: Dr. P. Ryan Steed

Abstract

As the primary producer of a cell's energy currency, adenosine triphosphate (ATP), F_1F_O ATP synthase is essential for life on this planet. Using the H^+ gradient across a membrane, the F_o complex generates torque on the F_1 complex, which synthesizes ATP. However, aspects of F_o functionality, including the functional interactions between subunit *a* (stator) and the c_{10} ring (rotor) remain unresolved. Through site-directed mutagenesis and chemical modifications we found that Phe 54 on subunit *c* (cF54) acts as a hydrophobic barrier preventing protons from leaking into the cytoplasm. cF54 also ensures that the c-subunit is positioned correctly in the membrane. While conducting these experiments, we found that an artificial histidine (His) tag on the a-subunit was influencing our results due to its presence in the exit channel and close proximity to cF54. A species of glacial ice worm has been found to possess a His rich sequence in the same location, with possible effects on ATP synthase function. Using an ATP synthase luminescence assay, we tested the effects of removing the His tag from the a-subunit and replacing it with the M.solifugus sequence. Through transgenic mutagenesis of an *E. coli* plasmid, it has been found that this His rich domain is sufficient to increase ATP synthesis in *E. coli*. These results show that the effect of His tags on the proteins to which they are attached is not innocuous and can lead to errors in the data that must be accounted for. Our results also show that a change in the positive charge density at the exit channel of the a-subunit can affect both ATP synthesis and hydrolysis.

1. Introduction

Adenosine triphosphate (ATP) is the principal energy currency of life (Figure 1). The energy released from hydrolysis of ATP is used as the thermodynamic driving force throughout various metabolic reactions.

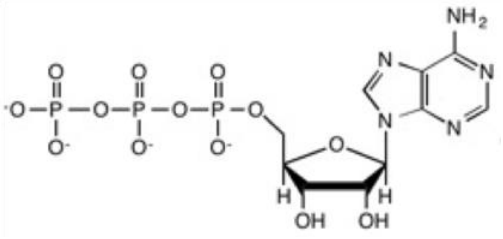

Figure 1. Adenosine Triphosphate

The primary source of ATP in all living organisms is F_1F_o ATP synthase (Figure 2). ATP Synthase is believed to be one of the oldest and most conserved enzymes in the history of life. It can be found in ancient organisms such as cyanobacteria where it is believed to have stayed in its current state with little to no change for billions of years[1].

F_1F_o ATP synthase is a membrane-bound transporter protein complex. It is driven by a proton (H^+) or sodium (Na^+) gradient (depending on the species), which is used to drive adenosine diphosphate (ADP) phosphorylation. As a result of glycolysis and the electron transport chain, in H^+-driven ATP synthase organisms, the pH of the periplasm is decreased, creating an electrochemical gradient that ATP synthase uses to drive ATP production. The F_1 complex of the ATP synthase in *E.coli* consists of five different subunits called α_3, β_3, δ, ε, and γ, while the F_o complex consist of the a, b, and c subunits (Figure 3). Whether each subunit is placed in the F_1 or F_o complex is dependent on if the subunit is membrane bound. The F_1 subunits sit above the membrane, while the F_0 subunits are found embedded within the membrane.

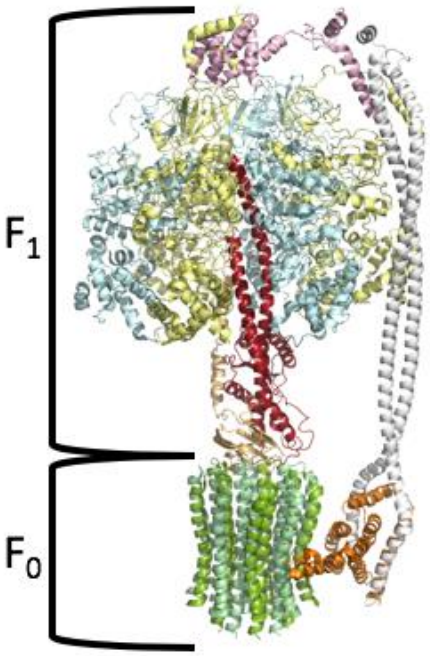

Figure 2. ATP Synthase F_1F_0.

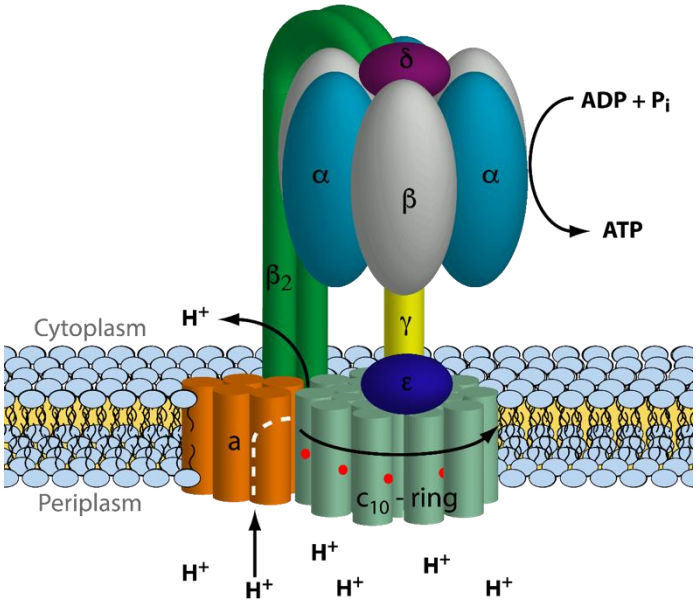

Figure 3. Subunits of ATP Synthase.

1.1 F_O Subcomplex

The a-subunit is composed of six α-helices, five of which are embedded in the membrane. The a-subunit provides H^+ with an aqueous pathway to and from the c-subunit. The c-subunit is a decamer, with each monomer composed of two α-helices joined by a hairpin turn (Figure 4 and 5). The monomers are joined together by intermolecular forces to form a ring structure. It is because of this ring structure that the c-subunit is often referred to as the c-ring. The monomers of the c-ring structure align themselves with the c1 α-helix toward the center of the ring and the c2 α-helix toward the outside of the ring. Each of the c2 α-helices contains an active/binding sites for H^+. Once H^+ ions bind to the c-ring, at the a-c interface on the periplasm side, the c-ring rotates around to the a-c interface on the cytoplasm side and deprotonates.

1.2 F_1 Subcomplex

The γ and ε subunits form a stalk that attaches to the center of the c-ring and to the center of the α-β complex. The stalk transfers the rotational energy of the c-ring to the α and β subunits. The three α and three β subunits alternate to form a hexameric complex that contains three active/binding sites of ADP and inorganic phosphate (P_i). The δ-subunit sits on the top of the α-β complex and with the b-subunit, stabilizes the F_1 complex. The b-subunit extends down into the membrane on the far side of the a-subunit from the c-ring. Another way to classify the twenty-two different subunits that make up ATP synthase, other than the F_1F_o division grouping, is by the rotor-stator model, in which the subunits are categorized by whether or not they rotate. Under this model, the c, γ, and ε are part of the rotor complex,

while the a, b, α, β, and δ are part of the stator complex. Researchers tend to use one or both of these models when talking about ATP synthase[2,3].

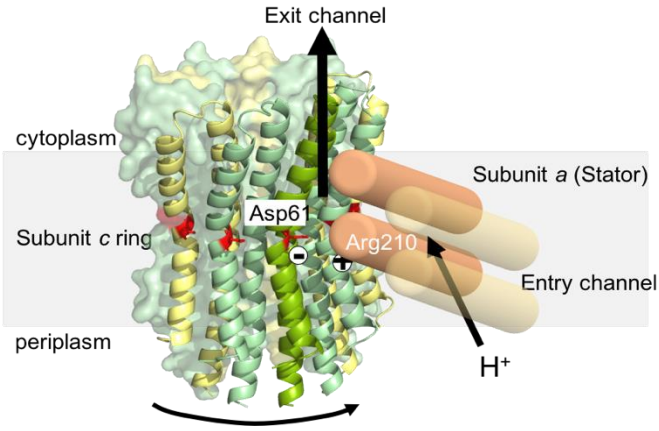

Figure 4. The a-c interface with Asp61 and Arg210 on the c and a-subunit respectively.

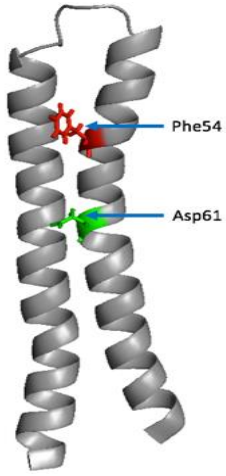

Figure 5. individual c-subunit with Phe54 and Asp61 on the c2 α-helix.

1.3 Background

Currently, the largest unknown surrounding ATP synthase deals with the mechanism by which ATP synthase turns a H^+ gradient into rotational motion. The reason why this mechanism is so perplexing is that the rotational motion is perpendicular to the H^+ gradient. Research within Dr. Steeds lab is primarily focused on a and c-subunit interactions. Various amino acid residues at the a-c interface have been found to be crucial to ATP synthase function. In order to test the import of these crucial residues, countless mutations have been made at the a-c interface. By replacing these residues with other amino acids, researchers have been able to determine the specific function of these residues. For instance, if a tyrosine was found to be important, mutagenesis would be used to test whether tyrosine was significant because of its aromaticity, its steric bulk, and/or its polar hydroxyl group. Subunit interaction is another aspect that these crucial residues are tested for. If researchers believe that certain residues on the a and c subunits are interacting with each other, they may replace the residues with cysteines in order to test whether or not the two cysteines are close enough to form a disulfide bond or a salt bridge.

Before a 2015 publication by Allegretti et al, the general consensus in the scientific community studying ATP synthase was that the α-helices of the a-subunit were parallel to the α-helices of the c-subunit. Diagrams throughout the literature showed the a-subunit as a group of transmembrane helices that stood vertical within the membrane. However, with a 6.2Å resolution cryo-electron microscopy image of the a-subunit Allegretti et al. discovered that the α-helices of the a-subunit were at a 20°-30° angle from the plane of the membrane and almost perpendicular to the α-helices of the c-subunit[4,11].

In a paper from 2008 by Steed and Fillingame, they reported that when the phenylalanine (Phe) residue, at the 54th position (Phe54) of the c-subunit transmembrane α-helix 2 (cTMH2) was genetically modified to a cysteine (F54C), ATP synthase was unable to pump protons across the membrane[12]. In order to determine why this was happening, we used chemical and genetic modifications to assess which properties of the Phe54 residue were crucial to *E.coli* ATP synthase function. The chemical modifications allowed us to test different side chains at the Phe54 site. We also used site directed mutagenesis to replace the Phe with an alanine (F54A), a valine (F54V), a leucine (F54L), an isoleucine, and a tyrosine (F54Y). The F54Y mutant allowed us to test whether Phe's lack of polarity was the key to its function. While the F54A, F54V, F54L, and F54I mutants, were used to test if steric bulk and hydrophobicity were the explanations. Function was determined through two different assays 1) ATP synthesis luminescence assay on inside out vesicles (ISOs) of *E.coli* 2) reverse H^+ pumping on ISOs of *E.coli*. The F_1F_o luminescence assay allows us to measure the synthesis function of the genetically modified ATP synthase compared to the wild type. Reverse H^+ pumping measures the hydrolysis function of the chemically and genetically modified ATP synthase compared to wild type.

The F54 residue of *E.coli* is positioned directly beneath the surface on the cytoplasm side of the cell membrane. Another Phe (Phe76) residue on the cTMH2 is situated beneath the surface on the periplasm side of the cell. Previous research by Preiss et al. on the ATP synthase of *Bacillus pseudofirmus* (*B.pseudofirmus*) reported that similar to *E.coli*, *B.pseudofirmus* had two Phe (Phe47, Phe69) residues on the cTMH2. Similar to *E.coli*, the Phe47 and Phe69 were positioned just beneath the surface of the cytoplasm and the periplasm respectively. Preiss et al. hypothesized that Phe47 and Phe69 formed the hydrophobic membrane boundary. We believe that this is also the case for Phe54 and Phe76 in *E.coli*[13].

While investigating the role of Phe54, we ran into problems with our site directed mutagenesis. Despite our continued attempts, successful mutations were few and far between. At the time our lab was using a plasmid called pCMA113, which had histidine (His) tags attached to the c-terminal region of subunit a and subunit β. These His tags were used by members of our lab for protein purification. However, these His tags had not been taken into account when designing the forward primer for PCR mutagenesis of UncE (gene that codes for the c-subunit). Within the Unc operon, the UncB gene, which codes for the a-subunit, is upstream of the UncE gene. As it turns out, the reason for our low mutagenesis success rate was due to the fact that the forward primer had a 9bp recognition sequence before the start of the His tag on the UncB gene and a 21bp recognition sequence after the His tag with 18bp unpaired in between. With this knowledge, we began using a plasmid called PVF2, which contained no His tag on the a-subunit. Our mutagenesis success rate increased significantly. Unfortunately, in order to ensure that all of our results were consistent, all old mutants had to be digested and transferred to the PFV2 plasmid.

Serendipitously, a paper was published around this same time by Lang et al. at Haverford college, which found increases in ATP concentration in a species of glacial ice worm known as *Mesenchytraeus solifugus.* Consequently, *M. solifugus* is the only *Mesenchytraeus* species that lives the entirety of its life at ~0^{o}C. The researchers showed that the increased concentration coincided with a His rich domain (VQDRSQAHSPVHAHSHGF) on the c-terminus end of the a-subunit that was not found in other species of the *Mesenchytraeus* genus. However, they offered no experimental evidence demonstrating that it was the His rich domain alone causing this increase. In their paper, they also mentioned 46 other species-specific mutations within *M. solifugus'* ATP synthase. They hypothesized that these mutations most likely contributed to increased ATP synthase efficiency at 0^{o}C but again offered no direct evidence for this claim[14].

In an earlier paper, by the same group, they found that while the His rich domain is novel among eukaryotes, similar His rich domains attached to various membrane transport proteins are found within various bacterial species. Lang and her team believe that *M. solifugus* may have acquired this domain through horizontal gene transfer (HGT) ~5-10mya[15].

If it is true that this His rich domain alone is responsible for increased efficiency of certain membrane transporter proteins in both eukaryotes and prokaryotes, then it should have a similar effect on bacterial ATP synthase. With this hypothesis, we set out to insert this same His rich domain into our His tag free PFV2 plasmid and insert it into our *E. coli* strain. In order to determine whether or not this domain is responsible for increased ATP production, we ran the same ATP synthesis luminescence assay that was performed on our Phe54 mutants.

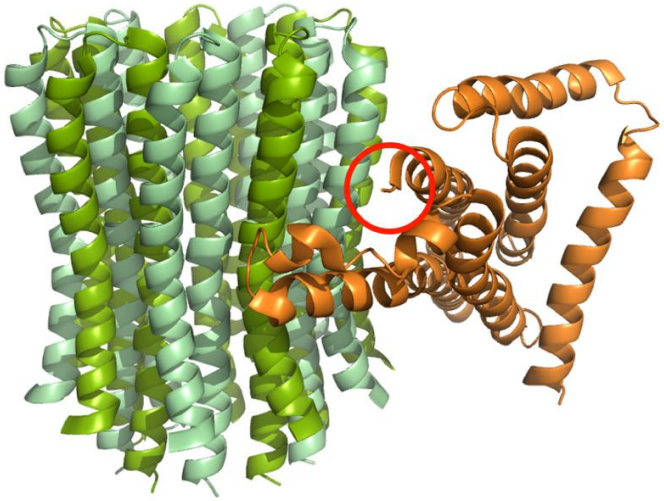

Figure 6. Showing where the His rich domian of M. solifugus is located (red ring). c-ring (green) and the a-sudunit (orange)

2. Materials and Methods

2.1 Site Directed Mutagenesis

Mutations were introduced using a 2-step megaprimer PCR method. PCR was carried out using a Bio-Rad T100 Thermal Cycler and New England Biolabs (NEB) Q5 High-Fidelity DNA Polymerase. A mutagenic primer and uncE_rev reverse end primer were used in the first step, and uncE_for forward end primer was used in the second step. Primers used in genetic modifications were obtained from Integrated DNA Technologies (IDT). PCR product

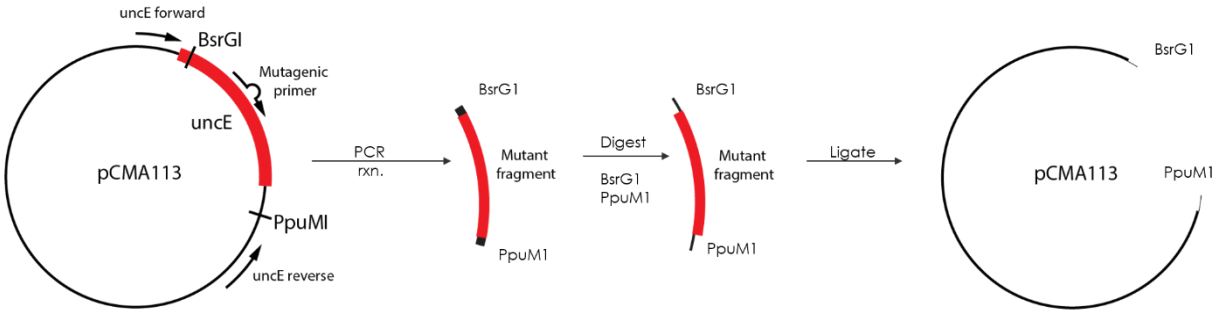

Figure 7. Outline of site directed mutagenesis

was purified using NEB Monarch PCR and DNA Cleanup Kit, and digested using BsrGI and PpuMI restriction enzymes. The digestion products were separated through 1% agarose gel electrophoresis with the insert and vector DNA isolated using NEB Monarch DNA Gel Extraction Kit. After extraction, DNA fragments were ligated using T4 DNA ligase. Competent cells from the DH5α cell line were transformed with the resulting plasmid. The cells were then placed on 100μg/mL ampicillin (amp) infused LB agar plates and incubated overnight at 37ºC. Colonies were collected from the plates and incubated overnight in 5mL of LB with 100 μg/mL amp. An aliquot of each sample was used to make a 12% glycerol stock, which was stored at -80ºC. The plasmid was purified using an NEB plasmid miniprep kit, and the presence of the mutation was confirmed by DNA sequencing. For functional assays, the mutant plasmid was introduced into the JWP292 cell line which contains no native F-ATP synthase[16].

2.2 Inside-out (ISO) and Stripped Vesicle Preparation

ISO vesicles were prepared by first growing transformed *E.coli* JWP292 cells in 1L of M63 minimal medium (a slow growth medium) containing 0.6% glucose, 0.2 mM uracil, 1 mM arginine, 2 μg/ml thiamine, 40 μM 2,3-dihydroxybenzoic acid, 100 μg/ml ampicillin, and 10% LB broth. M63 cultures were incubated overnight at 37^{o}C in a New Brunswick Scientific I2500 Series Incubator Shaker at 240 rpm. The cultures were centrifuged at 4000 x g for 15 minutes at 4^{o}C. The supernatant was decanted and cells were resuspended in TMG (50 mM Tris-HCl, 5 mM $MgCl_2$, 10% v/v glycerol, pH 7.5), with 1 mM DTT at 5mL per gram of cells. Cells were lysed using an Avestin EmulsiFlex-B15 homogenizer at 15,000 psi, and lysate was centrifuged at 9000 x g for 10 minutes at 4^{o}C. The supernatant was carefully transferred to an ultracentrifuge tube and centrifuged for 60 minutes at 193,000 x g at 4^{o}C. The pellet was then resuspended in 1mL per gram of cells of TMG. The protein concentration of ISO vesicles in solution was determined by a modified Lowry assay[17].

2.3 Chemical Modifications

Chemical modifications were done on the F54C mutant with derivatives of methanethiosufonate (MTS) reagents (Table 1). F54C ISO vesicles were diluted to 10mg/mL in TMG. Each MTS reagent was made to a concentration of 100 mM in dry DMSO and used to treat the F54C ISO vesicles at final concentration of 1-5 mM. N-ethylmaleimide at 5 mM in ethanol was also used to treat the F54C mutant.

Table 1. List Of Methanethiosulfonate Derivatives Used In Chemical Modification

Methanethiosulfonate derivatives	
Methyl	MMTS
Propyl	PMTS
Butyl	ButylMTS
Hexyl	HMTS
Tert-butyl ethyl	TertButylethylMTS
2-Carboxymethyl	MTSCE
4-Hydroxybenzyl	Ph-MTS
Benzyl	BenzylMTS
2-hydroxyethyl	MTSHE

2.4 ATP Hydrolysis Driven H^+ Pumping Assay

H^+ pumping activity was determined using fluorescence spectroscopy on an Aminco Bowman Series 2 Luminescence Spectrometer. F_1F_0 reverse H^+ pumping assay used 160μg of the ISO vesicles which was diluted in 3.2 mL of HMK (10 mM HEPES-KOH, 5.0 mM $MgCl_2$•6 H_2O, 300 mM KCl, pH 7.5) buffer with 8μL of 1.2mg/mL ACMA (9-Amino-6-Chloro-2-Methoxyacridine); (λ_{ex} = 415 nm, λ_{em} = 485 nm). Pumping was initiated with 30μL of 25mM ATP 20 s after the start of the assay, and nigericin was injected at 100 s.

2.5 ATP Synthesis Luminescence Assay

ATP synthase activity was measured using a Biotek Synergy HTX Multi-Mode Reader. The luminescence assay (Figure 8.) used 50 μg of ISO vesicles diluted with 50 μL of 2x reaction buffer, (Tricine 500mM/KOH pH 8, KCl 1M, $MgCl_2$ 200mM, HK_2PO_4 500mM, dIH_2O). 10 μL of 25mM NADH was added, just before reading, to the experimental solution and withheld from the control. dIH_2O was added to 100 μL. Within the wells of a 96 well plate (two wells per sample), 140 μL of 2x reaction buffer, 1 μL of 35.5 mM luciferin, 1 μL of 100ng/ μL luciferase, 12 μL 2.5mM ADP, and 126 μL dIH_2O. An initial background reading was taken. Followed by the addition and 1min incubation of

the NADH in the experimental tube. To their respective wells, 20 μL of both the control and experimental solutions were added. The photon emission of each well was measured every 20sec for 300sec.

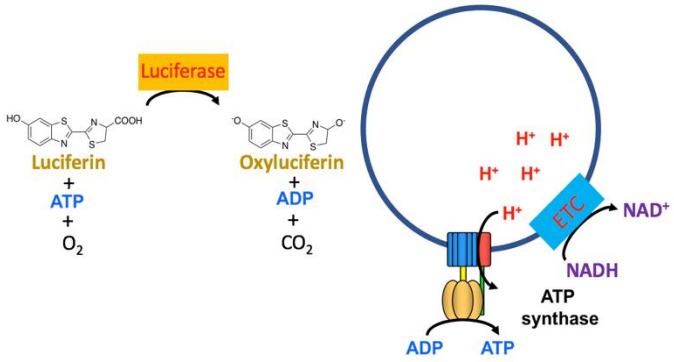

Figure 8. ATP Synthesis Assay

2.5 UncB With His Domain Mutagenesis

The *E. coli* UncB gene with the *M. solifugus* His rich domain was ordered from Integrated DNA Technologies (IDT) with a PflMI cut site at the 5' end and a BsrGI cut site at its 3' end. Both the PFV2 plasmid and the His modified UncB were digested using the BsrGI and PflMI restriction enzymes. The digest was run on a 1% agarose gel. The DNA fragments were cut from the gel and run through NEB Monarch DNA Gel Extraction Kit. The two fragments were then ligated together using T4 DNA Ligase. The plasmid was then transformed into DH5α competent cells using heat shock. The transformed cells were then plated on 100μg/mL ampicillin (amp) infused LB agar plates and incubated overnight at 37°C. Colonies were collected from the plates and incubated overnight in 5mL of LB with 100 μg/mL amp. The plasmid was purified using an NEB plasmid miniprep kit, and the presence of the mutation was confirmed by gel electrophoresis. For functional assays, the mutant plasmid was introduced into the DK8 cell line which contains no native F-ATP synthase.

3. Results

3.1 Chemical Modifications

In order to test which properties of Phe are responsible for its contribution to wild type ATP synthase function, chemical modifications were made. Eleven different MTS reagents were used, each with a different functional group (Table 1). Our plan was to first test what role hydrophobic, nonpolar, steric bulk played at this position. We started with methyl group (MMTS), which showed a >5% return of function, then a PMTS (>6%), a ButylMTS (>7%), HMTS (>20%), and finally a TertButylMTS (>7%). Each showed some return of function, with HMTS showing the greatest return. We then tested how polar groups attached to hydrophobic sterically bulky sidechains might affect function. We used an MTSHE (>16%) group, a MTSCE (>4%) group, and a Ph-MTS (>10%). Surprisingly, MTSHE showed the largest return of function of these polar groups and the third largest return of function overall. Unsurprisingly, the BenzylMTS, which most closely mimics the wild type phenylalanine, had the greatest return of function >25%.

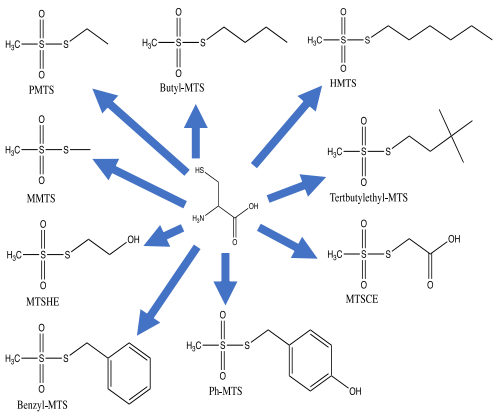

Figure 9. Structures of each methanethiosulfonate derivative used in chemical modification

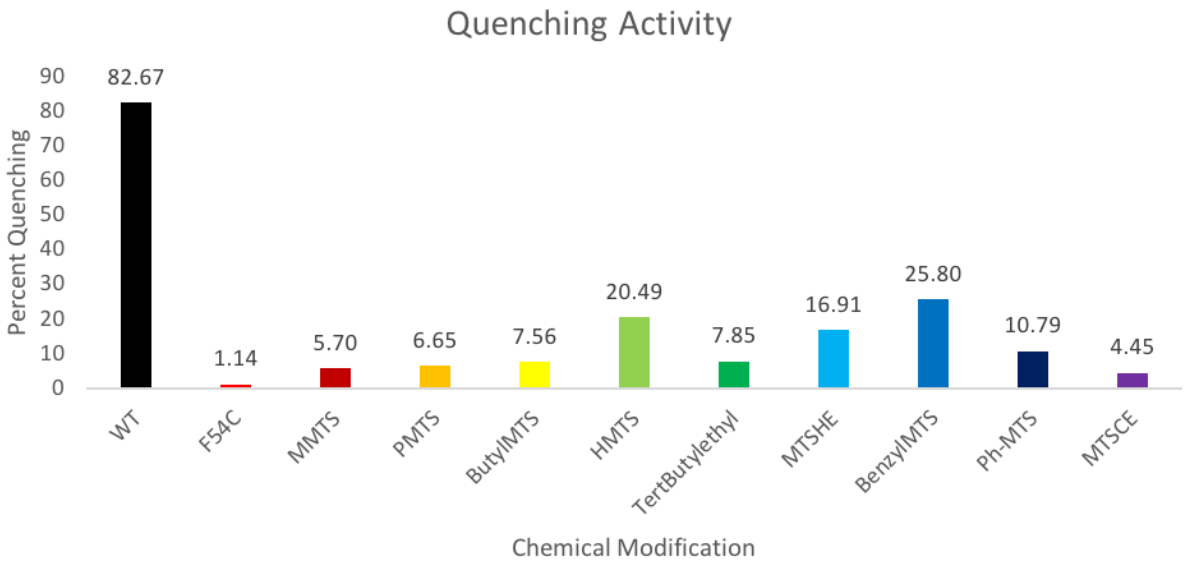

Figure 10. H^+ pumping activity indicated by percent quenching

3.2 Genetic Modifications

Our goal with the genetic modifications was similar to the chemical, we wanted to place residues at the 54 position that would test for steric bulk, hydrophobicity, polarity, and aromaticity. We began with the smallest hydrophobic residue alanine, which returned 33% of function, and then increased the steric bulk of the side chain with valine (85%), leucine (42%), and isoleucine (48%). Apart from the valine, this stepwise return of function was expected. We then created and tested a tyrosine (49%) mutant, that returned the same percent function as isoleucine. We believe the return was due to the polar hydroxy group of Tyr. Despite valines almost complete return of function, this valine was most likely still in the DH5α *E. coli* strain which contains multiple copies of the wild type plasmid. The cysteine (16%) mutant was created for the purposes of chemical modification.

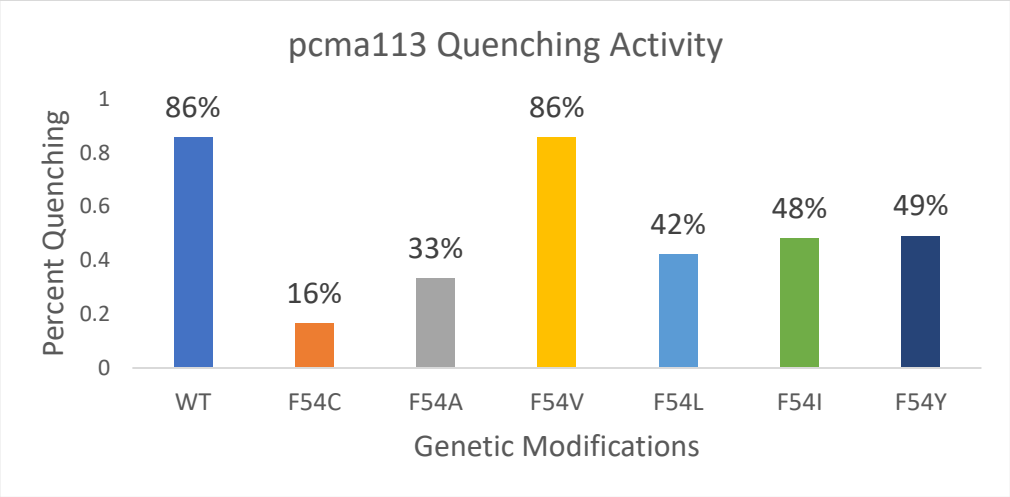

Figure 11. The percent quenching of pCMA113 genetically modified mutants compared to the wild type (wt).

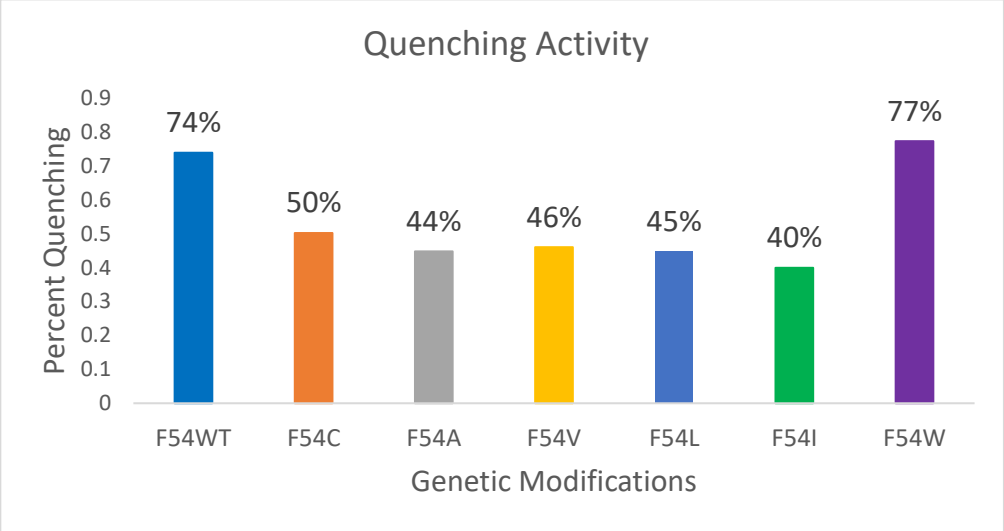

Figure 12. The percent quenching of PFV2 genetically modified mutants compared to the wild type (wt).

3.3 UncB Ice Worm Modification

In their 2020 paper, Lang et al. reported that *M. solifugus*, a species of glacial ice worm, showed a significant increase in ATP concentration compared to other species of the same genus. Lang and her colleges ascribed this increase to a His rich domain on the c-terminal end of the a-subunit. In order to determine whether or not this natural His tag is responsible for increased ATP production, we modified the UncB gene in our PFV2 *E. coli* plasmid, to incorporate this natural His tag. ISO vesicles of this modified *E. coli* were used in our luminescence assay (Figure 14). Figure 13 compares the average photon emissions for PFV2 modified (ICE) and unmodified (PFV2). The graph (Figure 13.) is based on the average initial rate of production looking at the first 80sec with measurements taken 20sec apart. PFV2 had an average initial rate of 13.4 $\pm$ 1.4 Lum/sec, while ICE had an average initial rate of 108.5 $\pm$ 30.7.

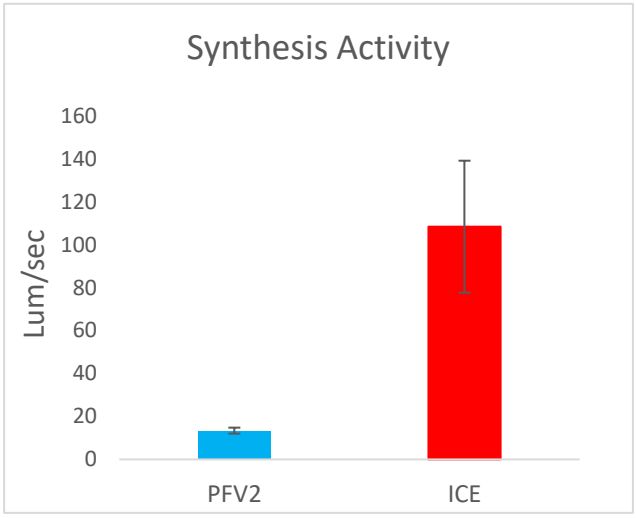

Figure 13. Luminescence assay, measuring the average initial rate of photon emissions over the first 80sec from PFV2 and UncB + His domain (ICE) ISO vesicles

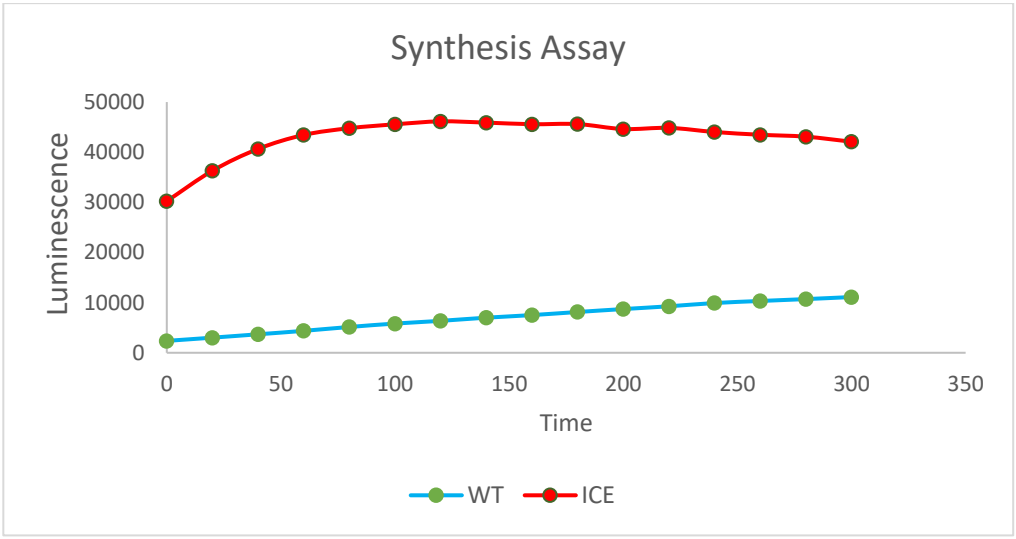

Figure 14. Synthesis assay, measuring photon emissions over 300sec from PFV2 and UncB + His domain (ICE) ISO vesicles

4. Conclusions

We observed a correlation between the return of functionality to ATP synthase and the properties of steric bulk and hydrophobicity at position 54. Despite the F54V aberration, we are seeing a stepwise return of function as hydrophobic steric bulk is returned. We hypothesize that the return of function seen with the polar side chains, in both the chemically modified (MTSHE >16%) and the genetically modified (Tyr >48%) groups, are a result of the snorkeling effect, which happens when the hydrophilic groups within a side chain positions themselves outside of the hydrophobic membrane region while the hydrophobic groups remain buried in the membrane. In order to test this hypothesis, we plan to create tryptophan, threonine, and serine mutations.

As stated by Preiss et al, we believe that cF54 acts as a hydrophobic membrane boundary. The reason we see such a dramatic reduction in function when Phe54 is mutated to Cys54 has to do with the proper alignment of the a and c-subunits. As the most sterically bulky hydrophobic side chain of the essential amino acids, Phe is ideal for stabilizing the c-ring within the membrane. When these properties are reduced or a polar group is added, this causes the c-ring to shift toward the cytoplasm causing a misalignment of the a and c-subunits. The misalignment may also allow protons to leak from the entry channel into the exit channel. Essentially causing a short circuit of the electrochemical gradient.

Additional mutants will narrow the key characteristics essential to the F54 site. These along with the current mutants will need to be run though H^+ permeability assays. Moving forward, all mutants need to be run through luciferin assays and H^+ pumping assays of stripped vesicles. We are also interested in the cooperative role that I55 and F54 seem to have. ATP synthase also shows an almost complete loss of function when mutated to I55C. Due to its sterics and hydrophobicity we believe that I55 plays a similar role as Phe54. So, we plan to do a double alanine mutant and an I55F/F54I mutant to get a better picture of how these two residues are interacting. We predict that this double mutant should behave very similarly to the wild type due to the retained hydrophobic nature at these positions.

The massive disparity in ATP synthesis between the His modified and unmodified a-subunit in PFV2 shows direct evidence that the *M. solifugus'* His rich domain is responsible for the increased ATP concentration seen in the research of Lang et al. This is consistent with other, ongoing (unpublished), research in Dr. Steeds lab. We have observed evidence of increased ATP hydrolysis when comparing pCMA113 and PFV2 mutants especially cysteine (Figure 11 and 12). We have also seen a decrease in synthesis activity in our cT51V mutation. Both of these phenomena are associated with a change in the positive charge density in the F_o exit channel. The His rich domain of *M. solifugus* most likely increases the positive charge density which leads to decreased binding affinity on proton binding sites in the exit channel. The same is probable true for the artificial His tag on the a-subunit in pCMA113. This might be why we see such a dramatic difference between the pCMA113 and PFV2 F54C mutants. The cT51V mutation, however, shows evidence of a decrease in the positive charge density which would explain its decreased in synthesis activity. Future research should focus on determining the structure of the *M. solifugus* His domain at this location. The structure would offer insight into how this His domain is interacting with the environment near the exit channel. It would also be interesting to insert the entire *M. solifugus* ATP synthase into an *E. coli* strain and perform synthesis assays on *M. solifugus* ATP synthase with and without the His domain and at various temperatures. This would determine whether or not the other mutations, noted by Lang et al, are actually involved in increases in efficiency at temperatures around 0^oC as well as a much more accurate representation of the increased production of ATP by the *M. solifugus* ATP synthase. Finally, a luminescence assay could be used to determine the reaction rate of the *M. solifugus* ATP synthase.

5. Works Cited

1) Kühlbrandt, W.; Davies, K. M. Rotary ATP synthases: A New Twist to an Ancient Machine. *Trends in Biochemical Sciences* **2016**, *41* (1), 106–116.
2) von Ballmoos, C.; Wiedenmann, A.; Dimroth, P. Essentials for ATP Synthesis by $F_1 F_0$ ATP Synthases. *Annual Review of Biochemistry* **2009**, *78* (1), 649–672.
3) Pogoryelov, D.; Krah, A.; Langer, J. D.; Yildiz, Ö.; Faraldo-Gómez, J. D.; Meier, T. Microscopic Rotary Mechanism of Ion Translocation in the Fo Complex of ATP Synthases. *Nature Chemical Biology* **2010**, *6* (12), 891–899.
4) Allegretti, M. et al. (2015) Horizontal membrane-intrinsic /-helices in the stator a-subunit of an F-type ATP synthase. Nature 521, 237–240 23.
5) Fillingame, R. H.; Steed, P. R. Half Channels Mediating H+ Transport and the Mechanism of Gating in the Fo Sector of Escherichia Coli F1Fo ATP Synthase. *Biochimica et Biophysica Acta (BBA) - Bioenergetics* **2014**, *1837* (7), 1063–1068.
6) Jiang, W.; Fillingame, R. H. Interacting Helical Faces of Subunits a and c in the F1Fo ATP Synthase of Escherichia Coli Defined by Disulfide Cross-Linking. *Proceedings of the National Academy of Sciences* **1998**, *95* (12), 6607–6612.
7) Yanagisawa, S.; Frasch, W. D. Protonation-Dependent Stepped Rotation of the F-Type ATP Synthase c-Ring Observed by Single-Molecule Measurements. *Journal of Biological Chemistry* **2017**, *292* (41), 17093–17100.
8) Martin, J.; Hudson, J.; Hornung, T.; Frasch, W. D. F_o-Driven Rotation in the ATP Synthase Direction against the Force of F_1 ATP synthase in the $F_o F_1$ ATP Synthase. *Journal of Biological Chemistry* **2015**, *290* (17), 10717–10728.
9) Sobti, M.; Smits, C.; Wong, A. S.; Ishmukhametov, R.; Stock, D.; Sandin, S.; Stewart, A. G. Cryo-EM Structures of the Autoinhibited E. Coli ATP Synthase in Three Rotational States. *eLife* **2016**, *5*.

10) Pierson, H. E.; Kaler, M.; O'Grady, C.; Uhlemann, E.-M. E.; Dmitriev, O. Y. Engineered Protein Model of the ATP Synthase H+- Channel Shows No Salt Bridge at the Rotor-Stator Interface. *Scientific Reports* **2018**, *8* (1).
11) Srivastava, A. P.; Luo, M.; Zhou, W.; Symersky, J.; Bai, D.; Chambers, M. G.; Faraldo-Gómez, J. D.; Liao, M.; Mueller, D. M. High-Resolution Cryo-EM Analysis of the Yeast ATP Synthase in a Lipid Membrane. *Science* **2018**, *360* (6389), eaas9699.
12) Steed, P. R.; Fillingame, R. H. Subunit *a* Facilitates Aqueous Access to a Membrane-Embedded Region of Subunit *c* in *Escherichia Coli* $F_1 F_0$ ATP Synthase. *Journal of Biological Chemistry* **2008**, *283* (18), 12365–12372.
13) Preiss, L.; Langer, J. D.; Yildiz, Ö.; Eckhardt-Strelau, L.; Guillemont, J. E. G.; Koul, A.; Meier, T. Structure of the Mycobacterial ATP Synthase Fo Rotor Ring in Complex with the Anti-TB Drug Bedaquiline. *Sci. Adv.***2015**, *1*(4), 1–9.
14) Lang, S. A.; McIlroy, P.; Shain, D. H. Structural Evolution of the Glacier Ice Worm Fo ATP Synthase Complex. *Protein J.* **2020**, No. 0123456789. https://doi.org/10.1007/s10930-020-09889-x.
15) Lang, S. A.; Shain, D. H. Atypical Evolution of the F 1 F o Adenosine Triphosphate Synthase Regulatory ATP6 Subunit in Glacier Ice Worms (Annelida: Clitellata: Mesenchytraeus). *Evol. Bioinforma.* **2018**, *14*. https://doi.org/10.1177/1176934318788076.
16) Barik, S. (1996). Site-directed mutagenesis in vitro by megaprimer PCR. *Methods in Molecular Biology (Clifton, N.J.), 57*, 203-215.
17) Fillingame, R. H. (1976). Purification of the carbodiimide reactive protein component of the ATP energy transducing system of Escherichia coli. *Journal of Biological Chemistry*, *251*(21), 6630–6637.